

Pressure–Temperature Dependence of Polymer Segmental Dynamics. Comparison between the Adam–Gibbs Approach and Density Scalings

Gustavo A. Schwartz,^{*,†} Juan Colmenero,^{†,‡} and Ángel Alegría[‡]

Donostia International Physics Center, Paseo Manuel de Lardizabal 4, 20018 San Sebastián, Spain, and Departamento de Física de Materiales UPV/EHU, Unidad de Física de Materiales CSIC-UPV/EHU, Facultad de Química, Apartado 1072, 20080 San Sebastián, Spain

Received November 16, 2005; Revised Manuscript Received February 23, 2006

ABSTRACT: By means of dielectric spectroscopy, the segmental dynamics (α -relaxation) of four different polymers (poly(vinyl acetate), poly(vinyl methyl ether), poly(vinyl chloride) and poly(*o*-chlorostyrene)) was measured over a broad range of frequencies (10^{-1} – 10^7 Hz), pressures (0–300 MPa), and temperatures (240–460 K). Two different approaches were used to analyze the temperature–pressure dependence of the relaxation time: a pressure-extended Adam–Gibbs equation ($\tau(T,P) = \tau_0 \exp[C/(TS_c(T,P))]$) and a particular density scaling ($\log(\tau) \propto f(TV^\gamma)$), both recently proposed. Both approaches give an excellent description of the experimental data; however, an inconsistency between them was found. We show that other scaling laws can give an equally good description of the experimental data, being therefore possible to improve the consistency between the density scaling and the AG framework.

1. Introduction

The problem of the glass transition has been in the focus of the debate for decades, and it is an important open question in condensed matter physics in general and of polymer science in particular. Historically, the study of the molecular dynamics approaching the glassy state was restricted to mainly analyze the effect of temperature. Thus, measurements of the relaxation time (at atmospheric pressure) as a function of temperature were performed in order to get information about molecular motions. Although much has been learned from these studies, it is not possible to separate thermal and density effects only by varying the temperature. However, the glass transition can also be approached by applying high enough pressure to a supercooled liquid. Both the increase of pressure and the decrease of temperature result in slower molecular motions. These two different ways of approaching the glass transition allow decoupling thermal and volumetric effects. Some of the seminal works in the study of the pressure effects on molecular dynamics of glass-formers were done in the 1960s,^{1–3} and a renewed interest has arisen during the past years.^{4–10} The improvement of the experimental techniques has made possible to obtain large amount of accurate data over broader ranges of pressure, temperature, and frequency and therefore contributes to the better understanding of the involved processes.

In the past years mainly two different approaches have been used to analyze the pressure–temperature dependence of the relaxation times of glass-forming systems. One is based on the Adam–Gibbs (AG) theory¹¹ and was developed by Casalini et al.⁵ They have recently proposed an extended AG equation to describe the behavior of the structural relaxation time, τ , as a function of both pressure and temperature. This equation was derived from the AG theory by writing the configurational entropy, S_c , in terms of the excess of both thermal heat capacity and thermal expansion. The second approach is based on a

density scaling^{12,13} ($\log(\tau) \propto f(TV^\gamma)$, γ being a material constant) which superposes into a single master curve the experimental data measured at different pressures and temperatures. The material specific constant (γ) has been empirically determined for several glass-formers, including a few polymers, and has also been related to the ratio of the activation enthalpy at constant volume to that at constant pressure.¹² More recently, Roland et al.¹⁴ have proposed a way to calculate the parameter γ only from equation-of-state (EOS) data, without performing any relaxation measurement. Since both approaches have given so far an excellent description of the experimental data, there could be some connection between them. This is a point that has not been yet explored and which could suggest new hints for the mechanisms of the glass transition.

In this work the α -relaxation of four polymers was studied using broad-band dielectric spectroscopy (10^{-2} – 10^7 Hz) over a wide temperature range and pressures up to 300 MPa. The temperature–pressure dependence of the experimental relaxation times was found to be very well described using both the extended AG equation, with thermal and expansion coefficients determined from calorimetric and PVT data, respectively, and the previously mentioned density scaling. A connection between both approaches has been explored, showing that the proposed scaling (TV^γ) and the AG frame are not completely consistent within the ranges of pressures and temperatures here explored. We show that a new density scaling provides not only an equivalent excellent description of the experimental data but also a better consistency between both approaches.

2. Theoretical Background

We first briefly summarize the main points of the two approaches we will use in this work to analyze the pressure–temperature dependence of the segmental relaxation time of the four polymers. For a more detailed explanation the reader is invited to look the references below mentioned.

Adam–Gibbs Theory. The Adam–Gibbs (AG) theory, which is based on the assumption of cooperative rearranging regions, gives an expression that relates the increase of structural

[†] Donostia International Physics Center.

[‡] Unidad de Física de Materiales CSIC–UPV/EHU.

* Corresponding author: Tel +34 943 015389; Fax +34 943 015600; e-mail schwartz@sw.ehu.es.

relaxation time, τ , to the reduction of configurational entropy, S_c , by¹¹

$$\tau = \tau_0 \exp\left(\frac{C}{TS_c}\right) \quad (1)$$

where τ_0 is the value of τ at very high temperature and C is a material constant. This quantity is here assumed independent of temperature and pressure, although this assumption has been recently questioned.¹⁵ Since S_c is not experimentally accessible, it is usually identified with the excess entropy ($S_c \propto S_{ex} = S_{melt} - S_{crystal}$). Although some findings seem to suggest a general validity of the proportionality between S_{ex} and S_c , the physical meaning of this assumption is still under debate, and no general agreement has been achieved.^{16–18} Under this assumption the proportionality constant between S_{ex} and S_c (g_T) will only affect the value of C in eq 1. Thus, S_c , at atmospheric pressure, can be estimated as

$$S_c(T) = g_T S_{ex}(T) = g_T \int_{T_K}^T \frac{\Delta C_p(T')}{T'} dT' \quad (2)$$

where $\Delta C_p = C_p^{melt} - C_p^{crystal}$ is the excess heat capacity at atmospheric pressure and T_K is the Kauzmann temperature, which used to be of the order of $T_g - 50$ K, where the excess entropy would vanish. If an inverse temperature dependence is assumed for ΔC_p ($\Delta C_p = K/T$), the empirical Vogel–Fulcher–Tammann (VFT) equation¹⁹ ($\tau(T) = \tau_0 \exp(DT_0/(T - T_0))$) is recovered (with $T_0 = T_K$). However, this temperature dependence for ΔC_p is not always valid, and a linear dependence of ΔC_p with temperature is often a better approximation.²⁰

Recently, Casalini et al.⁵ have proposed an extension of eq 2 for the configurational entropy (S_c) by adding a term related to the pressure change. Thus, the temperature and pressure dependence of the S_c is given by

$$S_c(T,P) = g_T \int_{T_K}^T \frac{\Delta C_p(T')}{T'} dT' - g_P(T) \int_0^P \Delta\left(\frac{\partial V}{\partial T}\right)_{P'} dP' \quad (3)$$

where $\Delta(\partial V/\partial T)_P = \Delta(\partial V/\partial T)_P^{melt} - \Delta(\partial V/\partial T)_P^{crystal}$ is the difference of the thermal expansivity of the melt and the crystal; if g_P does not depend on temperature, then the thermal and volumetric contributions to the configurational entropy are fully decoupled.

It is worth noting here that S_{ex} and $\Delta(\partial V/\partial T)_P$ are defined as the difference between the corresponding quantity of the melt with respect to that of the crystal. However, it is sometimes impossible in polymers to get the thermodynamic properties of the crystalline state. In these cases, it is usually assumed that the heat capacity and thermal expansion for the crystal are similar to those of the glass.²¹ Thus, we have used for calculations $\Delta C_p \cong C_p^{melt} - C_p^{glass}$ and $\Delta(\partial V/\partial T)_P \cong \Delta(\partial V/\partial T)_P^{melt} - \Delta(\partial V/\partial T)_P^{glass}$.

The AG theory and their assumptions are still under debate, and no general agreement about them has been yet achieved. However, the general agreement between the experimental results and the theory is good enough to assume that the model is, at least, plausible.^{22,23}

Density Scaling. In the past years Tölle et al.²⁴ have shown, based on the analysis of inelastic neutron scattering data under high pressure, that *o*-terphenyl (OTP) behaves like a soft-spheres system with a repulsive potential r^{-12} . This assumption leads to a description of the relaxation time for the OTP in terms of a single variable TV ,⁴ where V is the specific volume (expressed in cm^3/g). Later, Dreyfus et al.²⁵ found that light-scattering data for OTP can also be rescaled into a single master curve when

plotted as a function of TV .⁴ However, strong deviations from the proposed TV scaling were recently found in other systems.^{12,13} They showed that for several glass-formers the logarithm of the main (or α -) relaxation time, measured at various temperatures and pressures, yields a master curve when plotted against TV^γ , where γ is a material-specific constant which was found to vary in the range $0.14 \leq \gamma \leq 8.5$ for the glass-formers investigated to date.

The parameter γ provides a measure of the relative importance of V compared to T in the glass-forming dynamics. It is immediately clear that $\gamma = 0$ means a pure thermally controlled dynamics; on the other hand, for the hard-spheres limit, $\gamma \rightarrow \infty$ and the dynamics becomes entirely volume dependent. According to Casalini et al.,¹² it is therefore expected that γ correlates with the ratio of the activation enthalpy at constant volume $E_V = R[\partial \log(\tau)/\partial(T^{-1})]_V$ to that at constant pressure $E_P = R[\partial \log(\tau)/\partial(T^{-1})]_P$, E_V/E_P evaluated at T_g . Figure 3 in ref 12 shows the correlation between γ and E_V/E_P for several glass-formers. Recently, Roland et al.¹⁴ have shown that the parameter γ “can be calculated from EOS data alone, without recourse to actual relaxation measurements”; they also extensively discuss the physical meaning of the parameter γ .

3. Experimental Section

Samples. Four different polymers, having a wide range of T_g s, were used for this study: poly(vinyl acetate) (PVAc: $[\text{C}_4\text{H}_6\text{O}_2]_n$, $M_w = 93\,080$ g/mol, $M_n = 33\,200$ g/mol); poly(vinyl methyl ether) (PVME: $[\text{C}_3\text{H}_6\text{O}]_n$, $M_w = 21\,900$ g/mol, $M_n = 7\,300$ g/mol); deuterated poly(vinyl chloride) (PVCd: $[\text{C}_2\text{D}_3\text{Cl}]_n$, $M_w = 70\,000$ g/mol, $M_n = 35\,000$ g/mol); and poly(*o*-chlorostyrene) (PoClS: $[\text{C}_8\text{H}_7\text{Cl}]_n$, $M_w = 225\,000$ g/mol, $M_n = 132\,000$ g/mol). Deuterated PVC was chosen because it is more stable at high temperatures, and it is therefore possible to measure it within the full temperature range without a significant effect of sample degradation.

Differential Scanning Calorimetry (DSC). As mentioned in the previous section, we need to know $\Delta C_p = C_p^{melt} - C_p^{glass}$ as a function of the temperature for each polymer in order to estimate the excess entropy. As shown in Figure 1, the heat capacity can be well described by a linear function both above and below T_g (this is valid for the four polymers investigated). Thus, the excess heat capacity (ΔC_p) can be expressed according to the empirical linear equation $\Delta C_p = b - m_T T$. Calorimetric measurements were performed on PVME and PoClS by using a Q1000 TA Instruments DSC in the modulated mode, using different periods, with amplitude of 0.5 K and underlying cooling rate of 0.1 K/min. We have observed an excellent reproducibility (within 3%) by repeating the measurements several times on the same sample and on different samples of the same polymer. By varying the period of modulation, an extrapolation to zero frequency can be made, and thus the quasi-static value of C_p be determined for each polymer. Figure 1 shows the heat capacity for PoClS at three different periods. For each curve a set of values for b and m_T were obtained. The inset shows the extrapolation of b and m_T to zero frequency. The extrapolations were done using empirical functions due to the lack of an appropriate theoretical frame. Table 1 shows the corresponding values of b and m_T for all polymers. Heat capacity data for PVAc and PVCd were taken from refs 26 and 27, respectively, and correspond to quasi-static values (equivalent to zero extrapolated values) of the heat capacity; the corresponding values of b and m_T are also shown in Table 1.

Pressure–Volume–Temperature (PVT) Measurements. To calculate the volumetric contribution to the configurational entropy, we need to estimate $\Delta(\partial V/\partial T)_P$. The temperature dependence of the volume was measured with PVT 100 SWO/Thermo Haake equipment, for PVCd and PoClS, at different pressures (20–250 MPa) and temperatures between 30 and 140 °C (and 200 °C), respectively. The corresponding parameters for PVT data are shown in Table 2. Some curves for PVCd are shown in the inset of Figure

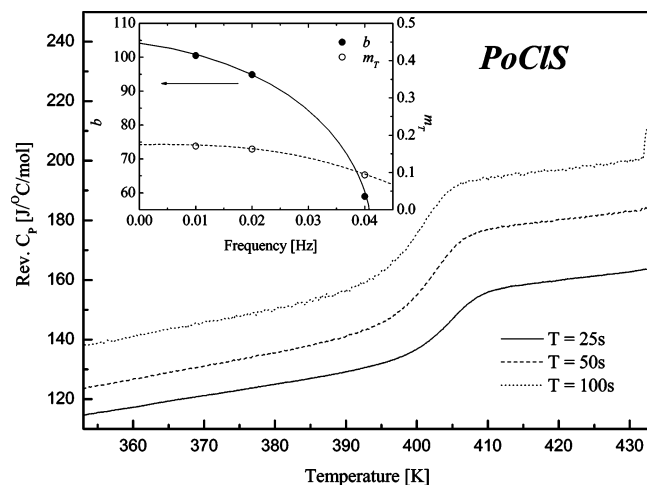


Figure 1. Reversible heat capacity against temperature, for PoClIS, as obtained from modulated DSC at different periods. The curves were shifted vertically for clarity. Heat capacity above and below T_g was approximated by a linear function, and thus ΔC_p ($\Delta C_p = b - m_T T$) was estimated at each frequency. The inset shows the extrapolation of b and m_T to zero frequency to estimate the quasi-static value of ΔC_p as a function of the temperature. The lines in the inset are a guide for the eye.

Table 1. Parameters of the Linear Function Used To Approximate ΔC_p According to $\Delta C_p = b - m_T T$

polymer	b [J K ⁻¹ mol ⁻¹]	m_T [J K ⁻² mol ⁻¹]	T_g [K]
PVAc ^c	104 ± 1	0.21 ± 0.01	308 ± 1
PVME ^b	68.3 ± 0.5	0.16 ± 0.01	247 ± 1
PVCd ^c	-48.3 ± 0.4	-0.20 ± 0.01	355 ± 1
PoClIS ^b	103 ± 1	0.17 ± 0.01	402 ± 1

^a Calorimetric T_g (at the inflection point) for all the here-studied polymers are also listed. Errors come from the linear fitting procedure. ^b Values extrapolated to zero frequency from modulated DSC measurements. ^c Quasi-static values calculated from the heat capacity data from refs 26 and 27.

Table 2. Parameters of the Empirical Function $V(P,T) = K_1/(P + K_4) + K_2 T/(P + K_3)$ Used To Describe PVT Data for Both Glassy and Melt States^a

polymer	state	K_1 [cm ³ MPa/g]	K_2 [cm ³ MPa/g °C]	K_3 [MPa]	K_4 [MPa]
PVCd	glass	1380 ± 15	0.275 ± 0.005	301 ± 5	1943 ± 15
	melt	1183 ± 12	2.735 ± 0.015	871 ± 9	1701 ± 15
PoClIS	glass	1651 ± 16	0.391 ± 0.005	556 ± 5	1988 ± 15
	melt	1575 ± 14	1.478 ± 0.015	365 ± 4	1986 ± 15

^a Errors come from the nonlinear fitting procedure.

2; from this plot we estimated $\Delta(\partial V/\partial T)_P$ by subtracting the slopes of the $V(T)$ curves above and below T_g . Figure 2 shows the pressure dependence of $\Delta(\partial V/\partial T)_P$ so obtained and the best fits to an empirical equation as described below. For PVAc the temperature dependence of the volume was estimated by plotting the specific volume, as given in ref 28, vs temperature and taking the slopes below and above T_g ; for the different pressures the Tait equation²⁸ was used with the parameters reported in ref 29 for the glassy state. Finally, values of $\Delta(\partial V/\partial T)_P$ as a function of pressure for PVME were taken from Figure 3.12 in ref 30. The data for these last two polymers are also shown in Figure 2.

For all the here studied polymers the pressure dependence of $\Delta(\partial V/\partial T)_P$ was described empirically according to

$$\Delta(\partial V/\partial T)_P = \Delta(\partial V/\partial T)_{P=0} - A[1 - \exp(-P/P_0)] \quad (4)$$

Table 3 shows the corresponding parameters.

Dielectric Measurements under Pressure. Dielectric measurements were carried out in a pressure cell (0–300 MPa) supplied by Novocontrol GmbH. The cell, basically a steel cylinder with a hermetic seal, is filled with a fluid which transmits the pressure

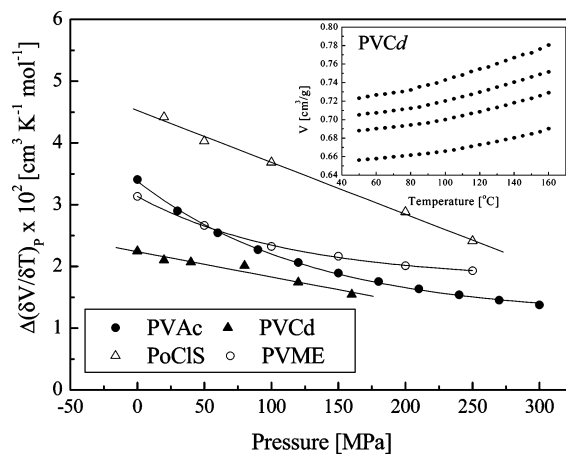


Figure 2. Pressure dependence of $\Delta(\partial V/\partial T)_P$ for all the here-studied polymers. An empirical exponential function was used to fit the experimental data (solid lines), and the corresponding parameters are listed in Table 3. The inset shows the raw specific volume vs temperature data for PVCd. For clarity, only some pressures are shown; from top to bottom 0, 40, 80, and 160 MPa.

Table 3. Parameters of the Empirical Exponential Function Used To Describe the Pressure Dependence of $\Delta(\partial V/\partial T)_P$ ^a

polymer	$\Delta(\partial V/\partial T)_{P=0} \times 10^2$ [cm ³ K ⁻¹ mol ⁻¹]	$A \times 10^2$ [cm ³ K ⁻¹ mol ⁻¹]	P_0 [MPa]
PVAc	3.35 ± 0.02	2.15 ± 0.04	129 ± 5
PVME	3.13 ± 0.02	1.31 ± 0.02	114 ± 5
PVCd	2.09 ± 0.02	12.6 ± 1.4	2996 ± 54
PoClIS	4.46 ± 0.02	24.6 ± 0.9	2797 ± 67

^a Errors come from the nonlinear fitting procedure.

from the piston to the sample. The sample consists of a very thin disk, 20 mm diameter and 0.1 mm thickness, placed between two gold-plated electrodes. The dielectric loss was measured in the whole frequency range (10^{-2} – 10^6 Hz) with a broad-band Alpha dielectric analyzer (Novocontrol GmbH). The measurements were performed by frequency sweeps at constant temperature, after stabilizing the temperature of the cell for about 2 h, with stability better than ± 0.1 K, and constant pressure, with stability better than ± 2 MPa. After each frequency sweep the pressure was changed, at constant temperature, to the next value, and once the highest value was reached, the pressure was reduced to the atmospheric value and temperature was changed. The measurements have shown a very good reproducibility after repeating them several times.

4. Results

Dielectric Relaxation Spectra. Figure 3a shows the dielectric loss (ϵ'') for PVAc, as a function of frequency, under atmospheric pressure, at different temperatures as determined using the pressure cell. Isothermal spectra, at various pressures, are shown in Figure 3b. Similar spectra were obtained for the other polymers. The central part of the main peak (i.e., the α -relaxation) was described using the Havriliak–Negami (HN) function

$$\epsilon^*(\omega) - \epsilon_\infty = \frac{\Delta\epsilon}{[1 + (i\omega\tau_{HN})^\alpha]^\beta} \quad (5)$$

where $\Delta\epsilon$ is the relaxation strength, τ_{HN} is a relaxation time, and α and β are shape parameters. For the purposes of this work, the characteristic relaxation time will be that of maximal loss $\tau = \tau_{\max} (\tau_{\max} = \tau_{HN}(\sin(\alpha\pi/(2 + 2\beta)))^{-1/\beta}(\sin(\alpha\beta\pi/(2 + 2\beta)))^{1/\beta})$.³¹

Figure 4 shows the full width at half-maximum (fwhm) of the α -relaxation, determined from the corresponding fitting curves, as a function of the corresponding relaxation time for all the studied polymers at different temperatures and pressures.

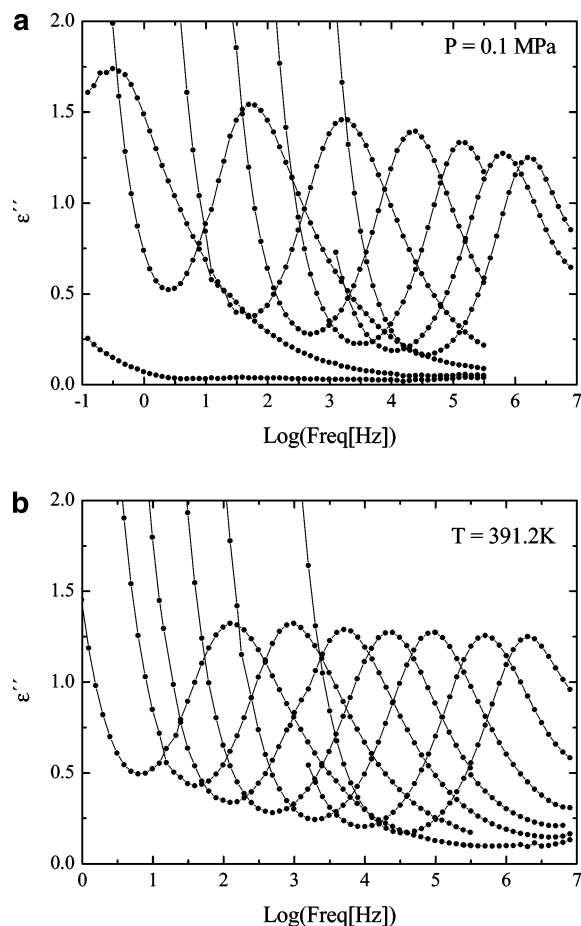


Figure 3. (a) Dielectric loss (ϵ'') for PVAc as a function of frequency, at atmospheric pressure, and different temperatures (from left to right: 300.5, 313.5, 326.4, 339.4, 352.3, 365.3, 378.3, and 391.2 K). (b) Dielectric loss (ϵ'') of PVAc, at 391.2 K, and different pressures (from left to right: 300, 250, 200, 150, 100, 50, and 0.1 MPa).

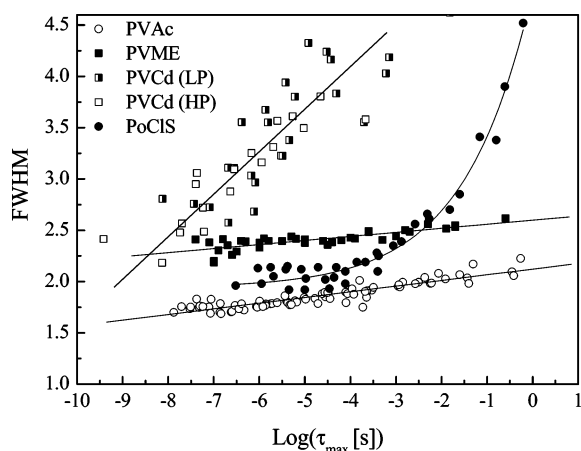


Figure 4. Full width at half-maximum of the α -relaxation peaks as a function of the corresponding characteristic relaxation time (τ_{\max}) obtained at different temperatures and pressures. For PVCd half-filled and empty squares represent the data at low and high pressures, respectively. Lines are a guide for the eye.

The fact that for each polymer all the points, obtained at different pressures and temperatures, collapse into a single line means that the shapes of the relaxation spectra and the relaxation time both depend on a single variable. In other words, the results depicted in Figure 4 evidence that the loss curves measured at different pressures and temperatures are hardly distinguishable when the comparison is made at the same value of the relaxation time. This behavior is in agreement with previous observa-

tions.^{8,32} Apart from PoClS, which will be commented on below, the fwhm increases almost linearly with increasing relaxation times. Although for PVCd the general tendency is also linear, a relatively big dispersion of the experimental data is observed. This is due to the anomalously broad spectra of PVCd which makes more difficult the accurate determination of the maximum and the fwhm. To show that no systematic pressure dependence is involved, the experimental data were plotted into two groups in Figure 4 (half-filled and empty squares for low and high pressures, respectively). It is clear that low- and high-pressure data are homogeneously distributed around the mean value (solid line).

Relaxation Times at Atmospheric Pressure. Figure 5 shows the temperature dependence of the maximum relaxation time, τ_{\max} , of the α -relaxation for all the polymers at different pressures. Filled and dashed lines represent the corresponding fits as explained below. The experimental data are in very good agreement with those previously published (see open symbols in Figure 5) by O'Reilly¹ and Heinrich and Stoll³³ for PVAc and PVC and by Casalini and Roland³² for PVME. Data on PoClS are here published, to the best of our knowledge, for the first time.

As mentioned in the previous section, we approximated the excess heat capacity (ΔC_p) to the empirical linear equation $\Delta C_p = b - m_T T$. According with this, the thermal contribution to the configurational entropy is

$$S_c(T, P \cong 0) = g_T \int_{T_K}^T \frac{\Delta C_p(T')}{T'} dT' = g_T (b \ln(T/T_K) - m_T(T - T_K)) \quad (6)$$

Thus, by introducing this result in eq 1, the temperature dependence of the relaxation time at atmospheric pressure is given by

$$\tau(T, P \cong 0) = \tau_0 \exp \left[\frac{C/g_T}{T(b \ln(T/T_K) - m_T(T - T_K))} \right] \quad (7)$$

By using eq 7 to fit the experimental data at atmospheric pressure, we got the three unknown parameters $\log(\tau_0[s])$, C/g_T , and T_K for all the here-studied polymers. Lowest solid lines in Figure 5 represent the best fit of eq 7 to the experimental data; the corresponding parameters are listed in Table 4.

Relaxation Times at Different Pressures. In the previous section we have estimated $\Delta(\partial V/\partial T)_P$ as a function of pressure, for the four polymers, and have described its pressure dependence by means of an empirical exponential function (eq 4). Now, we can estimate the pressure contribution to the configurational entropy as

$$g_P \int_0^P \Delta(\partial V/\partial T)_{P'} dP' = g_P [\Delta(\partial V/\partial T)_{P=0} P - A [P - P_0 (1 - \exp(-P/P_0))]] \quad (8)$$

By using eq 8 and eq 6 in eq 3 and then by replacing in eq 1, we obtain the following expression for the temperature–pressure dependence of the relaxation time

$$\tau(T, P) = \tau_0 \exp \left[\frac{C/g_T}{T \left\{ \left[b \ln \left(\frac{T}{T_K} \right) - m_T (T - T_K) \right] - \frac{g_P}{g_T} \left[\Delta \left(\frac{\partial V}{\partial T} \right)_{P=0} P - A \left[P - P_0 \left(1 - \exp \left(-\frac{P}{P_0} \right) \right) \right] \right] \right\}} \right] \quad (9)$$

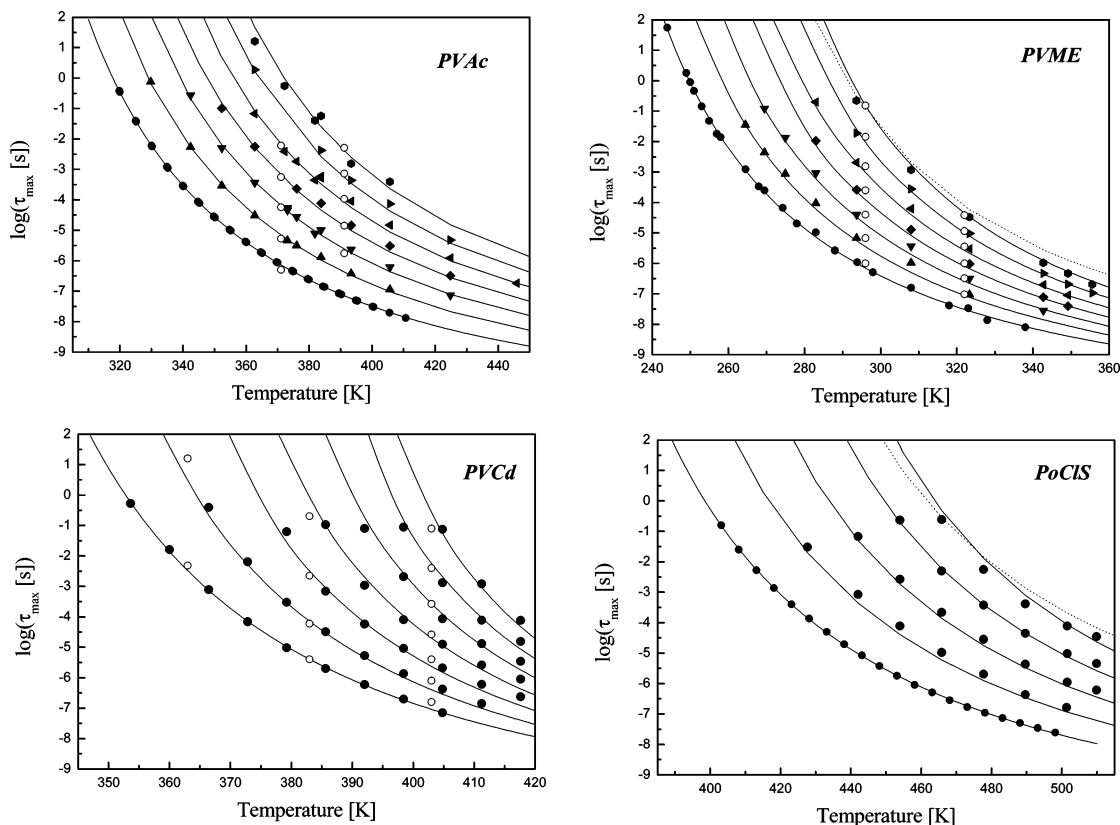


Figure 5. Temperature dependence of the relaxation time, for all the here-studied polymers, at different pressures (from bottom to top: $P_{\text{atm}} = 0.1, 50, 100, 150, 200, 250,$ and 300 MPa). For PoClS experimental data are available up to 200 MPa. Filled lines are the best fit of the experimental data by means of eq 9, with a constant g_P/g_T for PVCd and PVAc and a temperature-dependent g_P/g_T for PoClS and PVME, respectively. Dotted lines (only for PVME and PoClS at their highest pressure) are the best fit of eq 9 by keeping constant g_P/g_T (see text). Open circles represent some previously published experimental data points (PVAc, ref 1; PVME, ref 32; and PVC, ref 33).

Table 4. Parameters of the AG Model after Fitting the Experimental Data with Eq 7^a

polymer	$\log(\tau_0)$ [s]	C/g_T [J mol ⁻¹]	T_K [K]
PVAc	-14.1 ± 0.1	99094 ± 537	255.5 ± 0.2
PVME	-13.2 ± 0.1	54808 ± 2072	200.0 ± 1.0
PVCd	-11.2 ± 0.2	24338 ± 1186	301.5 ± 2.4
PoClS	-14.3 ± 0.1	111540 ± 3336	325.2 ± 1.3

^a Errors come from the nonlinear fitting procedure.

Note that the only unknown parameter in this equation is the ratio g_P/g_T . We have estimated it by minimizing the mean-square deviation between the experimental data and the relaxation times given by eq 9. It is worth mentioning that most of the parameters of eq 9 can be obtained from DSC and PVT characterization and from the temperature dependence of the relaxation times at atmospheric pressure through eq 7. The only free parameter which has to be obtained from measurements of the relaxation time at higher pressures is g_P/g_T . We have found in a recent work¹⁰ that a constant value of g_P/g_T in eq 9 gives an excellent description of the experimental data for PVAc (see upper-left plot in Figure 5). Thus, our first attempt was to calculate g_P/g_T for the different polymers by assuming a constant value. Besides the mentioned success for the PVAc, the pressure–temperature dependence of the relaxation time of PVCd can also be described with a constant value of g_P/g_T . Figure 5 shows the excellent agreement among experimental data and the predicted values (solid lines) for the relaxation times using eq 9. On the contrary, for PVME and PoClS a systematic deviation between the experimental and predicted points is observed. Dotted lines in Figure 5 are examples of such a deviation.

As pointed out in the Introduction, g_P could depend on temperature and therefore g_P/g_T could, too. By assuming a linear

Table 5. Calculated Values of g_P/g_T by Minimizing the Mean-Square Deviation between Experimental and Predicted Relaxation Times (Eq 9)^a

polymer	g_P/g_T	$(g_P/g_T)_{T_g}$	m_g [K ⁻¹]	γ	dT_g/dP [K GPa ⁻¹]
PVAc	1.05			2.2 ± 0.05	224 (250)
PVME	(0.71)	0.81	-1.6×10^{-3}	2.5 ± 0.05	170 (177)
PVCd	0.83			0.85 ± 0.05	242 (189)
PoClS	(0.76)	0.92	-1.8×10^{-3}	1.5 ± 0.05	362 (360) ^b

^a The second column shows the values of g_P/g_T by assuming a constant value. Columns three and four show the parameters of a linear temperature dependence for g_P/g_T according to $g_P/g_T = (g_P/g_T)_{T_g} + m_g(T - T_g)$. The fifth column lists the material-specific constant γ used for the thermodynamical scaling. The last column shows the calculated pressure coefficient of T_g in the limit of low pressure (the values in parentheses were taken from ref 14). ^b Upper limit for PS.¹⁴

dependence for g_P/g_T with temperature, we can write $g_P/g_T(T) = (g_P/g_T)_{T_g} + m_g(T - T_g)$ and estimate $(g_P/g_T)_{T_g}$ and m_g by minimizing the mean-square deviation as previously. The so-obtained parameters are listed in Table 5, together with those calculated by considering a constant value for g_P/g_T . Figure 5 shows the predicted values of the relaxation times (solid lines) for PoClS and PVME by using eq 9, and the proposed temperature linear dependence for g_P/g_T .

Density Scaling. Figure 6 shows the relaxation times for the four polymers, measured at different pressures and temperatures, as a function of TV^γ , where V represents the specific volume expressed in cm³/g. The parameter γ was adjusted for each polymer to yield a master curve with a minimum mean-square deviation. Table 5 shows the so-obtained values of γ ; for PVME the found value ($\gamma = 2.5$) is in very good agreement with those previously estimated $\gamma = 2.55$ ¹² and $\gamma = 2.7$.¹³ As shown in

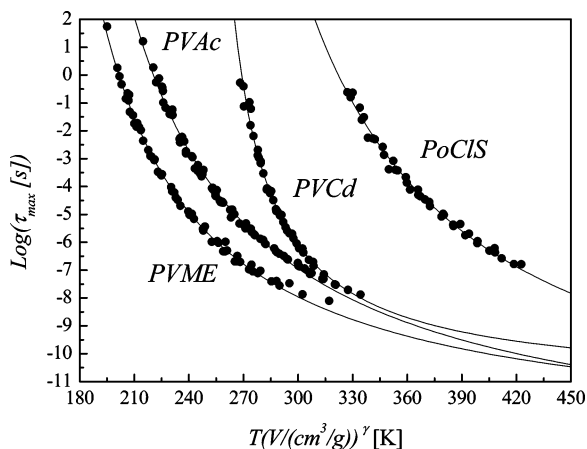


Figure 6. Maximum relaxation time, measured at different temperatures and pressures, as a function of TV^γ . The value of the parameter γ which gives the better master curve for each polymer is shown in Table 5.

Figure 6, the superposition is excellent for all the here studied polymers over a broad frequency range of more than 10 decades and for very different conditions of T and P . These findings are in agreement with all reported results in nonpolymer glass-forming systems, which evidence the general applicability of this scaling procedure.

5. Discussion

The temperature–pressure equivalence showed in Figure 4 for the here-studied polymers is in agreement with what is often observed for other glass-formers. Figure 4 indicates that the effects of pressure and temperature are hardly distinguishable when the comparison is made at the same value of the relaxation time. For PVAc and PVME most of the experimental points collapse into a single line, giving a rather linear correlation between fwhm and $\log(\tau)$. For PVCd we have already shown that despite the relatively big dispersion of the experimental data, a linear tendency is also observed. However, this is not the case for PoClIS; in this case a good superposition into a single line is observed, but the $\log(\tau)$ dependence of the fwhm is much stronger than in the previous cases. This fact together with other strange features of PoClIS like the anomalous pressure dependence of its relaxation strength is worth to be further deeply analyzed in a later work.

Although there is still no satisfactory explanation for the correlation between fwhm and $\log(\tau)$, an interpretation in terms of the coupling model has been recently proposed.³⁴ Anyway, it is clear from the experimental evidence that a single factor controls simultaneously the position and shape of the spectra. Thus, by predicting the relaxation time (at any pair T – P) we also know (through Figure 4) the shape of the corresponding relaxation spectrum. Therefore, we will in the following focus only on the description of the dependence of the relaxation times with pressure and temperature.

We have shown that the pressure-extended Adam–Gibbs model, by means of eq 9, gives an excellent description of the experimental data at any pressure or temperature (see Figure 5), with just one free parameter, g_p/g_T (beyond those three necessary to describe the data at atmospheric pressure) for PVAc and PVCd. This agreement between the experimental data and the proposed pressure-extended AG model strongly supports the validity of the AG framework and its assumptions. From the fitting procedure we found that for PVAc and PVCd a constant value of g_p/g_T is enough to give an outstanding description of the experimental data. This is in agreement with

Table 6. Parameters of the Generalized VFT Equation ($\tau(X) = \tau_0^{\text{AG}} \exp(DX_0/(X - X_0))$) after Fitting the Master Curves, with Different Scaling Laws, for the Here-Studied Polymers^a

polymer	$X = TV^\gamma$			$X = T(aV - 1)$			$X = T(a \log(V) + 1)$		
	γ	D	X_0 [K]	a	D	X_0 [K]	a	D	X_0 [K]
PVAc	2.2	19.2	138.5	2.2	19.0	172.8	3.7	19.2	146.6
PVME	2.5	14.4	136.7	1.8	14.4	110.3	4.8	14.4	138.9
PVCd	0.85	2.8	242.9	10	2.63	2650	1.5	2.6	254.3
PoClIS	1.5	16.1	216.6	3.7	15.8	596	2.7	15.7	225

^a The values of τ_0^{AG} are those obtained by using AG eq 7 and are listed in Table 4. The specific volume V is expressed in cm^3/g .

previous works^{9,10} where constant values of g_p/g_T ($0.7 < g_p/g_T < 1.1$) were also found for several polymers. However, the relaxation times of PVME and PoClIS could not be sufficiently well described by means of eq 9 with a constant value of g_p/g_T (see dashed lines in Figure 5). Instead, a linear temperature dependence for g_p/g_T was used giving an excellent fitting (with similar temperature coefficients for both polymers). This fact would mean that for these two polymers g_p depends on temperature, and therefore the thermal and volumetric contributions to the configurational entropy are not completely separated.

From the predicted values in Figure 5 (solid lines) we can estimate the dielectric glass transition temperature, T_g^{Diel} ($\tau(T_g^{\text{Diel}}) = 100$ s), for each polymer at different pressures. Thus, the pressure sensitivity, which quantifies the effect that pressure has on the dynamics, can be calculated as dT_g/dP . The last column in Table 5 shows the so-calculated pressure coefficients of T_g in the limit of low pressures. The values for PVAc and PVME are in excellent agreement with those previously published¹⁴ (see values in parentheses in last column of Table 5). The obtained value for deuterated PVC is higher than the corresponding value for protonated PVC¹⁴ probably due to differences in the microstructure (i.e., tacticity). For PoClIS there is no published data to compare with; however, the calculated pressure sensitivity is close to the upper limit for the polystyrene value (303 – 360 K GPa^{-1}).¹⁴ For the polymers analyzed in this work, we observed an increase of the average pressure sensitivity with the weight of the monomeric unit. Whether this evidences a general trend needs further work.

Concerning to the power density scaling of the relaxation time through a single variable of the form $X = TV^\gamma$, it has shown to be a simple and effective way to organize and display the large amount of isobaric and isothermal relaxation time data of glass-formers. The resulting master curves, for the here-studied polymers (Figure 6), can be well fitted with an empirical VFT-like equation given by

$$\tau(X) = \tau_0^{\text{AG}} \exp\left(\frac{DX_0}{X - X_0}\right) \quad (10)$$

where $X = TV^\gamma$, $X_0 = T_0V_0^\gamma$, and τ_0^{AG} is the relaxation time at high temperatures obtained by using AG eq 7 (and listed in Table 4). The parameter D is related to a generalized fragility m_x , defined following refs 12, 13 as the steepness of the $\log(\tau)$ vs X_g/X at X_g , through $m_x = d \log(\tau)/d(X_g/X)|_{X=X_g}$. It is clear that for $\gamma = 0$, i.e., a fully temperature-controlled process, the standard VFT equation is recovered. Solid lines in Figure 6 represent the best fit of the experimental data with eq 10, whereas the obtained parameters are listed in Table 6. A small deviation is observed in Figure 6 for some polymers when the relaxation time is faster than 10^{-7} s. This could be because we fixed τ_0 to that obtained by AG (eq 7), and it is well-known that the AG theory does not describe well the temperature behavior at short times, at least for small molecules.³⁵

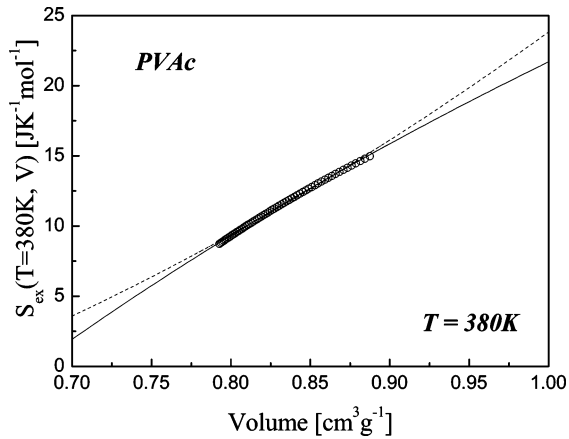


Figure 7. Excess entropy of PVAc, at constant temperature, as a function of the specific volume as obtained from calorimetric and PVT data. Dashed and solid lines represent the best fit of the excess entropy data according to $S_{\text{ex}}(V) = A(V^\gamma - 0.36)$ and $S_{\text{ex}}(V) = a \log(V) + B$, respectively (see text). Note the curvature of the experimental points and that of the power density scaling (dashed line) and logarithm density scaling (solid line).

Equation 10 can be rewritten in a different way according to

$$\tau(T,P) = \tau_0^{\text{AG}} \exp \left[\frac{DT_0}{T \left[\frac{V^\gamma}{V_0^\gamma} - \frac{T_0}{T} \right]} \right] \quad (11)$$

A direct comparison of this equation with the AG ones (eq 1) allows us to identify the configurational entropy with the bracket in the denominator of the exponential (in eq 11); thus, it follows

$$S_{\text{ex}}(T,V) \propto \left[\frac{V^\gamma}{V_0^\gamma} - \frac{T_0}{T} \right] \quad \text{or} \quad S_{\text{ex}}(T,V) \propto V^\gamma - \frac{X_0}{T} \quad (12)$$

This equation is particularly important since it relates the material-specific empirical parameter γ with fundamental quantities like the volume–temperature dependence of the configurational entropy. Thus, trying to test eq 12, we have plotted the excess entropy, obtained from thermodynamic and PVT data, at constant temperature, as a function of volume; Figure 7 shows the so-obtained excess entropy for PVAc at $T = 380$ K. The best fit of the experimental data with the equation $S_{\text{ex}}(T_{\text{const}}, V) = A(V^\gamma - B)$, leaving A , B , and γ as free parameters, gives $A = 83 \pm 15$ J/(mol K), $B = 0.7 \pm 0.1$, and $\gamma = 0.8 \pm 0.1$. These values are clearly inconsistent with those obtained from the dynamics through the power density scaling ($\gamma = 2.2$ and $B = 0.36$). The value of the exponent γ ($0 < \gamma < 1$) was not unexpected due to the curvature of the excess entropy. Similar results were obtained for the other three polymers. However, by fixing the value of B (X_0/T) to 0.36, obtained by fitting the PVAc data on Figure 6 with eq 10 (see Table 6), a value of $\gamma = 2.18 \pm 0.01$ is obtained (see dashed line in Figure 7). Although the fit (obtained from the dynamics through the TV^γ scaling) is a good approximation of the thermodynamics data, the functional forms of both descriptions are not equivalent because for all the polymers the excess entropy data show a systematic negative curvature (see Figure 7). This suggests that the Adam–Gibbs framework and the power density scaling (TV^γ) are not fully consistent, at least within the experimental window of pressures and temperatures here analyzed.

One important point to highlight here is that this density scaling (TV^γ) is not the only one which collapses the isobaric data at different pressures into a single master curve. Recently,

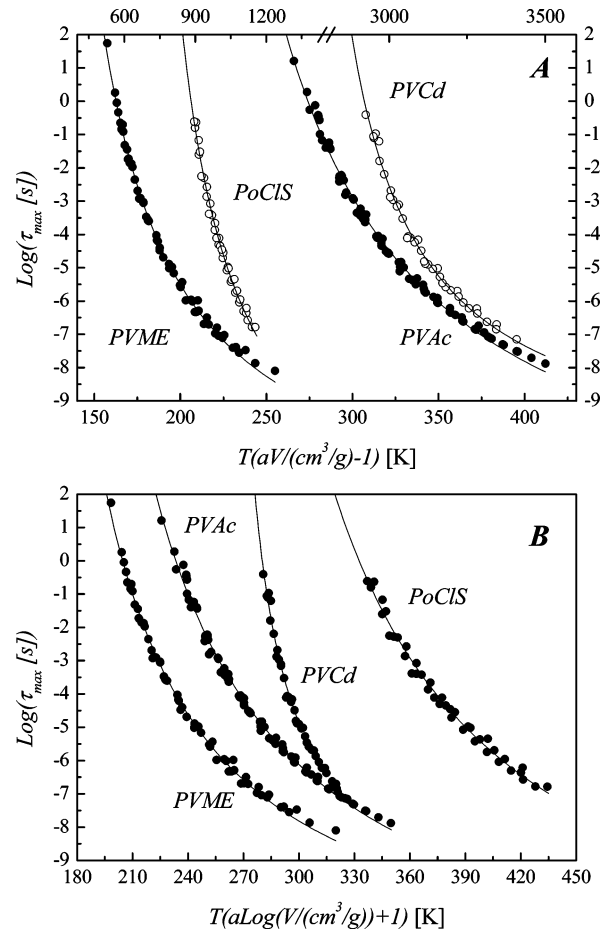


Figure 8. Master curves obtained for the four polymers by means of two different scaling: (A) $X = T(aV - 1)$ and (B) $X = T(a \log(V) + 1)$. In plot A filled and open symbols correspond to the lower and upper x axis, respectively. Filled lines represent, in both plots, the best fit of the experimental data by means of the equation $\tau(X) = \tau_0^{\text{AG}} \exp(DX_0/(X - X_0))$.

Alba-Simionescu et al.¹³ have shown that a linear density scaling ($X = T(aV - 1)$) works as well as the TV^γ one, at least for a limited range of P and T ; over larger ranges of T and P the linear scaling could fail as shown in ref 14. Figure 8a shows the relaxation time as a function of $X = T(aV - 1)$ for the four polymers. Solid lines represent the best fit to the experimental data with eq 10, whereas the so-obtained parameters are listed in Table 6. It is worth noting in this table that the fragility parameter (D), given in eq 10, is specific to the material dynamics and independent of the chosen density scaling and of the P – T path.

On the basis of the curvature of the thermodynamic points in Figure 7, we tested a logarithm density scaling defined as $X = T(a \log(V) + 1)$, which gives both an excellent overlapping of the dynamic data into a single master curve (see Figure 8b) and, as will be shown in the following, a better consistency with the AG frame. The generalized VFT parameters for this scaling are also listed in Table 6. In this case, eq 10 can be written as

$$\tau(T,P) = \tau_0^{\text{AG}} \exp \left[\frac{DX_0}{T \left[a \log(V) + 1 - \frac{X_0}{T} \right]} \right] \quad (13)$$

whereas eq 1 can be written as

$$\tau(T,P) = \tau_0^{\text{AG}} \exp\left[\frac{C/g_T}{TS_{\text{ex}}(T,P)}\right] \quad (14)$$

A comparison between eq 13 and 14 gives $S_{\text{ex}}(T,P) \propto a \log(V) + 1 - X_0/T$, which is valid for the whole range of pressures and temperatures. At constant temperature, and for the range of interest, we can approximate the volume dependence of the excess entropy by $S_{\text{ex}}(T_{\text{const}}, V(P, T_{\text{const}})) = A \log(V) + B$, based only on thermodynamic and PVT data. In particular, for PVAc at 380 K, the best fit of the experimental data gives $A = 127.7 \pm 0.5 \text{ J/(mol K)}$ and $B = 21.7 \pm 0.2 \text{ J/(mol K)}$ (solid line in Figure 7). We can now calculate these parameters from the dynamics data to test the consistency. Equations 13 and 14 lead to $A = (aC/g_T)/DX_0$ and $B = (C/g_T)/DX_0(1 - (X_0)/(T_{\text{const}}))$. The values of C/g_T are listed in Table 4, whereas the values of D and X_0 can be obtained by fitting the corresponding master curve with eq 10 (solid lines in Figure 8b); the values of a were obtained from the scaling and are listed in Table 6. The values of A and B so obtained (from dynamics data) are $A = 128.5 \pm 0.7 \text{ J/(mol K)}$ and $B = 21.6 \pm 0.4 \text{ J/(mol K)}$, which are in excellent agreement with those obtained from the fit of the thermodynamic data. Similar results were obtained for the other polymers. Thus, we have a very good consistency between the AG approach and the logarithm density scaling here analyzed. This is of particular relevance because it implies that the parameter of the density scaling, and therefore the relaxation time at any temperature and pressure, could be obtained from the PVT and thermodynamic data and the dynamics data at a given pressure and different temperatures. Furthermore, the logarithm scaling could be used as a way to test the AG approach over broader temperatures and pressures ranges. Nevertheless, this kind of test would require accurate PVT measurements at higher pressures which are not yet available.

6. Conclusions

We have analyzed in this work the temperature–pressure dependence of the relaxation times of four glass-forming polymers. We have shown that an extension of the AG theory, which includes the effect of pressure, gives an excellent description of the experimental data. Additionally, a power density scaling ($\log(\tau) \propto f(TV^\nu)$), which yields a superposition of different isobaric curves of the temperature dependence of the relaxation times, has also shown to give a very good description of the experimental data. However, we have shown that this scaling is not fully consistent with the Adam–Gibbs framework and that other scalings can also give an excellent description of the pressure–temperature dependence of the relaxation times. We have proposed a logarithm density scaling which not only works as well as that previously mentioned but also improves the consistency between both approaches. Although it is still not clear what the more appropriate density scaling law is, it is expected that further works on other glass-forming systems and broader ranges of pressure and temperature help to solve the question. Finally, it is worth noticing that the

generalized dynamic fragility given in eq 10 does not depend on the actual density scaling function.

Acknowledgment. This work has been supported in part by the Spanish Ministry of Science and Technology (MICyT) (project MAT 2004/01617) and by the Government of the Basque Country (project 9/UPV 00206.215-13568/2001). We want also thank Dr. Mertxe Fernandez for the PVT measurements on PVCd and PoCIS.

References and Notes

- O'Reilly, J. M. *J. Polym. Sci.* **1962**, *57*, 429.
- Williams, G. *Trans. Faraday Soc.* **1966**, *62*, 1321.
- Williams, G. *Trans. Faraday Soc.* **1966**, *62*, 2091.
- Corezzi, S.; Rolla, P. A.; Paluch, M.; Ziolo, J.; Fioretto, D. *Phys. Rev. E* **1999**, *60*, 4444.
- Casalini, R.; Capaccioli, S.; Lucchesi, M.; Rolla, P. A.; Corezzi, S. *Phys. Rev. E* **2001**, *63*, 031207.
- Prevosto, D.; Lucchesi, M.; Capaccioli, S.; Casalini, R.; Rolla, P. A. *Phys. Rev. B* **2003**, *67*, 174202.
- Roland, C. M.; Casalini, R. *Macromolecules* **2003**, *36*, 1361.
- Alegria, A.; Gomez, D.; Colmenero, J. *Macromolecules* **2002**, *35*, 2030.
- Prevosto, D.; Capaccioli, S.; Lucchesi, M.; Leporini, D.; Rolla, P. *J. Phys.: Condens. Matter* **2004**, *16*, 6597.
- Schwartz, G. A.; Tellechea, E.; Colmenero, J.; Alegría, A. *J. Non-Cryst. Solids* **2005**, *351*, 2616.
- Adam, G.; Gibbs, J. H. *J. Chem. Phys.* **1965**, *28*, 139.
- Casalini, R.; Roland, C. M. *Phys. Rev. E* **2004**, *69*, 062501.
- Alba-Simionesco, C.; Cailliaux, A.; Alegría, A.; Tarjus, G. *Europhys. Lett.* **2004**, *68*, 58.
- Roland, C. M.; Hensel-Bielowka, S.; Paluch, M.; Casalini, R. *Rep. Prog. Phys.* **2005**, *68*, 1405 and references therein.
- Johari, G. P. *J. Chem. Phys.* **2003**, *119*, 635.
- Angell, C. A.; Borick, S. J. *Non-Cryst. Solids* **2002**, *307–310*, 393 and references therein.
- Johari, G. P. *J. Non-Cryst. Solids* **2002**, *307–310*, 387.
- Johari, G. P. *J. Chem. Phys.* **2002**, *116*, 2043.
- Vogel, H. *Phys. Z* **1921**, *22*, 645. Fulcher, G. S. *J. Am. Ceram. Soc.* **1923**, *8*, 339. Tammann, G.; Hesse, W. *Z. Anorg. Allg. Chem.* **1926**, *156*, 245.
- Hodge, I. M. *Macromolecules* **1987**, *20*, 2897.
- Yamamuro, O.; Tsukushi, I.; Lindqvist, A.; Takahara, S.; Ishikawa, M.; Matsuo, T. *J. Phys. Chem. B* **1998**, *102*, 1605.
- Cangialosi, D.; Alegria, A.; Colmenero, J. *Europhys. Lett.* **2005**, *70*, 614.
- Goitiandia, L.; Alegria, A. *J. Chem. Phys.* **2004**, *121*, 1636.
- Tölle, A. *Rep. Prog. Phys.* **2001**, *64*, 1473.
- Dreyfus, C.; Aouadi, A.; Gapinski, J.; Matos-Lopes, M.; Steffen, W.; Patkowski, A.; Pick, R. M. *Phys. Rev. E* **2003**, *68*, 011204.
- ATHAS database, <http://web.utk.edu/~athas/databank/vinyl/pvac/pvac.html>; Gaur, U.; Wunderlich, B. *J. Phys. Chem. Ref. Data* **1981**, *10*, 1051. Gaur, U.; Wunderlich, B. B.; Wunderlich, B. *J. Phys. Chem. Ref. Data* **1983**, *12*, 29.
- ATHAS database, <http://web.utk.edu/~athas/databank/vinyl/pvc/pvc.html>; Loufakis, K.; Wunderlich, B. *Polymer* **1986**, *27*, 563.
- Mark, J. E. *Physical Properties of Polymers Handbook*; AIP Press: New York, 1996; Chapter 7.
- McKinney, J. E.; Simha, R. *Macromolecules* **1974**, *7*, 894.
- Chauty-Cailliaux, A. Ph.D. Thesis, University de Paris XI, France, 2003.
- Kremer, F.; Schönhals, A. *Broadband Dielectric Spectroscopy*; Springer-Verlag: Berlin, 2003; p 64.
- Casalini, R.; Roland, C. M. *J. Chem. Phys.* **2003**, *119*, 4052.
- Heinrich, W.; Stoll, B. *Colloid Polym. Sci.* **1985**, *263*, 873.
- Ngai, K. L.; Casalini, R.; Capaccioli, S.; Paluch, M.; Roland, C. M. *J. Phys. Chem. B* **2005**, *109*, 17356.
- Richert, R.; Angell, C. A. *J. Chem. Phys.* **1998**, *108*, 9016.

MA052464T